Shot noise of charge and spin transport in a junction with a precessing molecular spin

Milena Filipović and Wolfgang Belzig
Fachbereich Physik, Universität Konstanz, D-78457 Konstanz, Germany
(Dated: November 21, 2017)

Magnetic molecules and nanomagnets can be used to influence the electronic transport in mesoscopic junction. In a magnetic field the precessional motion leads to resonances in the dc- and ac-transport properties of a nanocontact, in which the electrons are coupled to the precession. Quantities like the dc-conductance or the ac-response provide valuable information like the level structure and the coupling parameters. Here, we address the current noise properties of such contacts. This encompasses the charge current and spin-torque shot noise, which both show a step-like behavior as functions of bias voltage and magnetic field. The charge current noise shows pronounced dips around the steps, which we trace back to interference effects of electron in quasienergy levels coupled by the molecular spin precession. We show that some components of the noise of the spin-torque currents are directly related to the Gilbert damping and, hence, are experimentally accessible. Our results show that the noise characteristics allow to investigate in more detail the coherence of spin transport in contacts containing magnetic molecules.

PACS numbers: 73.23.-b, 75.76.+j, 85.65.+h, 85.75.-d

I. INTRODUCTION

Shot noise of charge current has become an active research topic in the last decades, since it enables the investigation of microscopic transport properties, which cannot be obtained from the charge current or conductance.[1] Some of these properties result from the quantization of electron charge.[1] Namely, the nonequilibrium time-dependent fluctuations of charge current arise due to discrete nature of electron charge. Classical zero-frequency shot noise given by Schottky's formula $S(0) = e\langle I\rangle$ corresponds to uncorrelated charge carriers with Poissonian distribution.[2] Accordingly, the Fano factor defined as $F = S(0)/e\langle I\rangle$, which describes the deviation of the shot noise from the charge current, equals 1 in this case. In quantum devices the Fermi-Dirac distribution and the Pauli exclusion principle suppress ($F < 1$),[3–5] while the Coulomb interaction can either suppress ($F < 1$)[6,7] or enhance ($F > 1$)[8] the shot noise, depending on the system under consideration.

The quantum interference phenomenon, which is a manifestation of the wave nature of electrons, has attracted a lot of attention. The quantum interference effects occur between coherent electron waves in nanoscale junctions.[9] Quantum interference in molecular junctions influences their electronic properties.[10–14] The Fano effect[15] due to the interference between a discrete state and the continuum has an important role in investigation of the interference effects in nanojunctions, which behave in an analogous way, and are manifested in the conductance or noise spectra.[9,16,17] Particularly interesting examples involve spin-flip processes, like in the presence of Rashba spin-orbit interaction,[18,19] rotating magnetic field,[20] or in the case of the magnetotransport.[21–23]

It has been demonstrated that spin-flip induced fluctuations in diffusive conductors connected to ferromagnetic leads enhance the noise power, approaching the Poissonian value $F = 1$.[24] On the other hand, it has been shown that shot noise in a ferromagnet-quantum dot-ferromagnet system with antiparallel magnetization alignments can be suppressed due to spin-flip, with $F < 1/2$.[25] Shot noise can be used to study correlations of wave functions[26] and kinetics of electrons,[27] for example. Theoretically, shot noise has been mostly investigated in mesoscopic systems under dc-bias voltage. If the charge current is conserved, only current correlation at the same contact (auto-correlation noise) or between different contacts (cross-correlation noise) is needed to describe the shot noise of the system with two probes.[1] The cross-correlations take negative definite values for fermions.[3,28] The noise of charge current has been investigated using e.g., nonequilibrium Green's function method,[29–32] scattering matrix theory,[1] equation of motion method,[33] and Floquet master equation approach.[34]

In the domain of spin transport it is interesting to investigate the noise properties, as the discrete nature of electron spin leads to the correlations between spin-carrying particles. The spin current is usually a nonconserved quantity difficult to measure, and its shot noise depends on spin-flip processes leading to the spin-current correlations with opposite spins.[35–37] Consequently, in order to investigate the shot noise of spin current, one needs to study both auto-correlations and cross-correlations. The investigation of the spin-dependent scattering, spin accumulation[38] and attractive or repulsive interactions in mesoscopic systems can be obtained using shot noise of spin current,[39] as well as measuring the spin relaxation time.[35,39] Even in the absence of charge current, a nonzero spin current and its noise can still emerge.[37,40,41] Several works have studied shot noise of spin current using e.g., nonequilibrium Green's functions method and scattering matrix theory.[37,42–44]

It was demonstrated that the magnetization noise originates from transferred spin current noise via a fluctuating spin-transfer torque in ferromagnetic-normal-ferromagnetic systems,[45] and magnetic tunnel junctions.[46] Quantum noise generated from the scatterings between the magnetization of a nanomagnet and spin-polarized electrons has been shown as well.[47,48] The shot noise of spin-transfer torque has been recently studied using a magnetic quantum dot connected to two noncollinear magnetic contacts.[44] According to the definition of the spin-transfer torque,[49,50] both auto-correlations and cross-correlations of the spin-current components contribute to the spin-torque noise.

In this article we theoretically study noise of charge and spin currents and spin-transfer torque in a tunnel junction through which transport occurs via a single electronic energy level, in the presence of a molecular magnet in a constant magnetic field, connected to two normal metallic leads. The spin of the molecular magnet precesses around the magnetic field with Larmor frequency. Its precession is kept undamped by external sources. The electronic level may belong to a neighboring quantum dot or it may be an orbital of the molecular magnet itself. The electronic level and the molecular spin are coupled via exchange interaction. We derive expressions for the noise components using the Keldysh nonequilibrium Green's functions formalism.[51–53] The noise of charge current is contributed by both elastic processes driven by the bias voltage, and inelastic tunneling processes driven by the molecular spin precession. We observe dip-like features in the shot noise due to inelastic tunneling processes and destructive quantum interference between electron transport channels involved in the spin-flip processes. The driving mechanism of the correlations of the spin-torque components in the same spatial direction involves both precession of the molecular spin and the bias-voltage. Hence, they are contributed by elastic and inelastic processes, with the change of energy equal to one or two Larmor frequencies. The nonzero correlations of the perpendicular spin-torque components are driven by the molecular spin precession, with contributions of spin-flip tunneling processes only. These components are related to the previously obtained Gilbert damping coefficient,[54,55] which characterize the Gilbert damping term of the spin-transfer torque,[56–58] at arbitrary temperature.

The article is organized as follows. The model and theoretical framework based on the Keldysh nonequilibrium Green's functions formalism[51–53] are given in Sec. II. Here we derive expressions for the noise of spin and charge currents. In Sec. III we investigate and analyze the properties of the charge-current shot noise. This section is followed by Sec. IV in which we derive and analyze the noise of spin-transfer torque. The conclusions are given in Sec. V.

II. MODEL AND THEORETICAL FRAMEWORK

The junction under consideration consists of a noninteracting single-level quantum dot in the presence of a precessing molecular spin in a magnetic field along z-axis, $\vec{B} = B\vec{e}_z$, coupled with two noninteracting leads (Fig. 1). The junction is described by the Hamiltonian

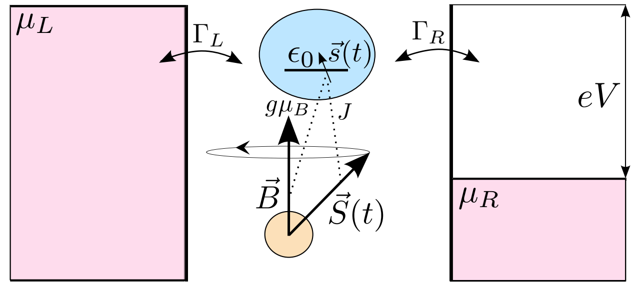

FIG. 1. (Color online) Tunneling through a single molecular level with energy ϵ_0 in the presence of a precessing molecular spin $\vec{S}(t)$ in a constant magnetic field $\vec{B}$, connected to two metallic leads with chemical potentials μ_ξ, $\xi = L, R$. The molecular level is coupled to the spin of the molecule via exchange interaction with the coupling constant J. The applied dc-bias voltage $eV = \mu_L - \mu_R$, and the tunnel rates are Γ_ξ.

$$\hat{H}(t) = \sum_{\xi\in\{L,R\}} \hat{H}_\xi + \hat{H}_T + \hat{H}_D(t) + \hat{H}_S, \tag{1}$$

where

$$\hat{H}_\xi = \sum_{k,\sigma} \epsilon_{k\xi}\hat{c}^\dagger_{k\sigma\xi}\hat{c}_{k\sigma\xi} \tag{2}$$

is the Hamiltonian of contact $\xi = L, R$. The spin (up or down) state of the electrons is denoted by the subscript $\sigma =\uparrow,\downarrow= 1, 2 = \pm1$. The tunnel coupling between the quantum dot and the leads reads

$$\hat{H}_T = \sum_{k,\sigma,\xi} [V_{k\xi}\hat{c}^\dagger_{k\sigma\xi}\hat{d}_\sigma + V^*_{k\xi}\hat{d}^\dagger_\sigma\hat{c}_{k\sigma\xi}], \tag{3}$$

with spin-independent matrix element $V_{k\xi}$. The creation (annihilation) operators of the electrons in the leads and the quantum dot are given by $\hat{c}^\dagger_{k\sigma\xi}(\hat{c}_{k\sigma\xi})$ and $\hat{d}^\dagger_\sigma(\hat{d}_\sigma)$. The Hamiltonian of the electronic level equals

$$\hat{H}_D(t) = \sum_\sigma \epsilon_0\hat{d}^\dagger_\sigma\hat{d}_\sigma + g\mu_B\hat{\vec{s}}\vec{B} + J\hat{\vec{s}}\vec{S}(t). \tag{4}$$

The first term in Eq. (4) is the Hamiltonian of the noninteracting single-level quantum dot with energy ϵ_0. The second term describes the electronic spin in the dot, $\hat{\vec{s}} = (\hbar/2)\sum_{\sigma\sigma'}(\vec{\sigma})_{\sigma\sigma'}\hat{d}^\dagger_\sigma\hat{d}_{\sigma'}$, in the presence of a constant magnetic field $\vec{B}$, and the third term represents the exchange interaction between the electronic spin and the molecular spin $\vec{S}(t)$. The vector of the Pauli matrices is given by $\hat{\vec{\sigma}} = (\hat{\sigma}_x, \hat{\sigma}_y, \hat{\sigma}_z)^T$. The gyromagnetic ratio of the electron and the Bohr magneton are g and μ_B, whereas J is the exchange coupling constant between the electronic and molecular spins.

The last term of Eq. (1) can be written as

$$\hat{H}_S = g\mu_B\vec{S}\vec{B}, \tag{5}$$

and represents the energy of the molecular spin $\vec{S}$ in the magnetic field $\vec{B}$. We assume that $|\vec{S}| \gg \hbar$ and neglecting quantum fluctuations treat $\vec{S}$ as a classical variable. The magnetic field $\vec{B}$ generates a torque on the spin $\vec{S}$, which causes the spin to precess around the field axis with Larmor frequency $\omega_L = g\mu_B B/\hbar$. The dynamics of the molecular spin is kept nondissipative by external sources (e.g., rf fields),[59] which cancel out the loss of its magnetic energy due to the interaction with the itinerant electrons. Thus, the precessing spin $\vec{S}(t)$ pumps spin-currents into the leads, but the spin-transfer torque exerted on the molecular spin is compensated by the above mentioned external means. The precessional motion of the molecular spin is then given by $\vec{S}(t) = S_\perp \cos(\omega_L t)\vec{e}_x + S_\perp \sin(\omega_L t)\vec{e}_y + S_z \vec{e}_z$, with θ the tilt angle between $\vec{B}$ and $\vec{S}$, and $S_\perp = S\sin(\theta)$ the magnitude of the instantaneous projection of $\vec{S}(t)$ onto the xy plane. The component of the molecular spin along the field axis equals $S_z = S\cos(\theta)$.

The charge and spin current operator of the lead ξ is given by the Heisenberg equation[51,52]

$$\hat{I}_{\xi\nu}(t) = q_\nu \frac{d\hat{N}_{\xi\nu}}{dt} = q_\nu \frac{i}{\hbar}[\hat{H}, \hat{N}_{\xi\nu}], \tag{6}$$

where $[\ ,\ ]$ denotes the commutator, while $\hat{N}_{L\nu} = \sum_{k,\sigma,\sigma'} \hat{c}^\dagger_{k\sigma L}(\sigma_\nu)_{\sigma\sigma'}\hat{c}_{k\sigma' L}$ is the charge ($\nu = 0$ and $q_0 = -e$) and spin ($\nu = x, y, z$ and $q_{\nu\neq 0} = \hbar/2$) occupation number operator of the contact ξ. Here $\hat{\sigma}_0 = \hat{1}$ is the identity matrix. Taking into account that only the tunneling Hamiltonian $\hat{H}_T$ generates a nonzero commutator in Eq. (6), the current operator $\hat{I}_{\xi\nu}(t)$ can be expressed as

$$\hat{I}_{\xi\nu}(t) = -q_\nu \frac{i}{\hbar}\sum_{\sigma,\sigma'}(\sigma_\nu)_{\sigma\sigma'}\hat{I}_{\xi,\sigma\sigma'}(t), \tag{7}$$

where the operator component $\hat{I}_{\xi,\sigma\sigma'}(t)$ equals

$$\hat{I}_{\xi,\sigma\sigma'}(t) = \sum_k [V_{k\xi}\hat{c}^\dagger_{k\sigma\xi}(t)\hat{d}_{\sigma'}(t) - V^*_{k\xi}\hat{d}^\dagger_\sigma(t)\hat{c}_{k\sigma'\xi}(t)]. \tag{8}$$

The nonsymmetrized noise of charge and spin current is defined as the correlation between fluctuations of currents $I_{\xi\nu}$ and $I_{\zeta\mu}$,[1,52]

$$S^{\nu\mu}_{\xi\zeta}(t,t') = \langle \delta\hat{I}_{\xi\nu}(t)\delta\hat{I}_{\zeta\mu}(t')\rangle, \tag{9}$$

with $\nu = \mu = 0$ for the charge current noise. The fluctuation operator of the charge and spin current in lead ξ is given by

$$\delta\hat{I}_{\xi\nu}(t) = \hat{I}_{\xi\nu}(t) - \langle\hat{I}_{\xi\nu}(t)\rangle. \tag{10}$$

Using Eqs. (7) and (10), the noise becomes

$$S^{\nu\mu}_{\xi\zeta}(t,t') = -\frac{q_\nu q_\mu}{\hbar^2}\sum_{\sigma\sigma'}\sum_{\lambda\eta}(\sigma_\nu)_{\sigma\sigma'}(\sigma_\mu)_{\lambda\eta}S^{\sigma\sigma',\lambda\eta}_{\xi\zeta}(t,t'), \tag{11}$$

where $S^{\sigma\sigma',\lambda\eta}_{\xi\zeta}(t,t') = \langle\delta\hat{I}_{\xi,\sigma\sigma'}(t)\delta\hat{I}_{\zeta,\lambda\eta}(t')\rangle$. The correlation functions $S^{\sigma\sigma',\lambda\eta}_{\xi\zeta}(t,t')$ can be expressed by means of the Wick's theorem[60] as

$$\begin{aligned} S^{\sigma\sigma',\lambda\eta}_{\xi\zeta}(t,t') = \sum_{kk'}[&V_{k\xi}V_{k'\zeta}G^>_{\sigma',k'\lambda\zeta}(t,t')G^<_{\eta,k\sigma\xi}(t',t) \\ &- V_{k\xi}V^*_{k'\zeta}G^>_{\sigma'\lambda}(t,t')G^<_{k'\eta\zeta,k\sigma\xi}(t',t) \\ &- V^*_{k\xi}V_{k'\zeta}G^>_{k\sigma'\xi,k'\lambda\zeta}(t,t')G^<_{\eta\sigma}(t',t) \\ &+ V^*_{k\xi}V^*_{k'\zeta}G^>_{k\sigma'\xi,\lambda}(t,t')G^<_{k'\eta\zeta,\sigma}(t',t)], \end{aligned} \tag{12}$$

with the mixed Green's functions defined, using units in which $\hbar = e = 1$, as

$$G^<_{\eta,k\sigma\xi}(t,t') = i\langle\hat{c}^\dagger_{k\sigma\xi}(t')\hat{d}_\eta(t)\rangle, \tag{13}$$

$$G^>_{\sigma',k'\lambda\zeta}(t,t') = -i\langle\hat{d}_{\sigma'}(t)\hat{c}^\dagger_{k'\lambda\zeta}(t')\rangle, \tag{14}$$

while Green's functions $G^<_{k\sigma\xi,\eta}(t,t') = -[G^<_{\eta,k\sigma\xi}(t',t)]^*$ and $G^>_{k'\lambda\zeta,\sigma'}(t,t') = -[G^>_{\sigma',k'\lambda\zeta}(t',t)]^*$. The Green's functions of the leads and the central region are defined as

$$G^<_{k\sigma\xi,k'\sigma'\zeta}(t,t') = i\langle\hat{c}^\dagger_{k'\sigma'\zeta}(t')\hat{c}_{k\sigma\xi}(t)\rangle, \tag{15}$$

$$G^>_{k\sigma\xi,k'\sigma'\zeta}(t,t') = -i\langle\hat{c}_{k\sigma\xi}(t)\hat{c}^\dagger_{k'\sigma'\zeta}(t')\rangle, \tag{16}$$

$$G^<_{\sigma\sigma'}(t,t') = i\langle\hat{d}^\dagger_{\sigma'}(t')\hat{d}_\sigma(t)\rangle, \tag{17}$$

$$G^>_{\sigma\sigma'}(t,t') = -i\langle\hat{d}_\sigma(t)\hat{d}^\dagger_{\sigma'}(t')\rangle, \tag{18}$$

$$G^{r,a}_{\sigma\sigma'}(t,t') = \mp i\theta(\pm t \mp t')\langle\{\hat{d}_\sigma(t), \hat{d}^\dagger_{\sigma'}(t')\}\rangle. \tag{19}$$

Since the self-energies originating from the coupling between the electronic level and the lead ξ are diagonal in the electron spin space, their entries can be written as $\Sigma^{<,>,r,a}_\xi(t,t') = \sum_k V_{k\xi}g^{<,>,r,a}_{k\xi}(t,t')V^*_{k\xi}$, where $g^{<,>,r,a}(t,t')$ are the Green's functions of the free electrons in lead ξ. Applying Langreth analytical continuation rules,[61] Eq. (12) transforms into

$$\begin{aligned} S^{\sigma\sigma',\lambda\eta}_{\xi\zeta}(t,t') = \int dt_1 \int dt_2 \{&[G^r_{\sigma'\lambda}(t,t_1)\Sigma^>_\zeta(t_1,t') \\ &+ G^>_{\sigma'\lambda}(t,t_1)\Sigma^a_\zeta(t_1,t')] \\ &\times [G^r_{\eta\sigma}(t',t_2)\Sigma^<_\xi(t_2,t) + G^<_{\eta\sigma}(t',t_2)\Sigma^a_\xi(t_2,t)] \\ &+ [\Sigma^>_\xi(t,t_1)G^a_{\sigma'\lambda}(t_1,t') + \Sigma^r_\xi(t,t_1)G^>_{\sigma'\lambda}(t_1,t')] \\ &\times [\Sigma^<_\zeta(t',t_2)G^a_{\eta\sigma}(t_2,t) + \Sigma^r_\zeta(t',t_2)G^<_{\eta\sigma}(t_2,t)] \\ &- G^>_{\sigma'\lambda}(t,t')[\Sigma^r_\zeta(t',t_1)G^r_{\eta\sigma}(t_1,t_2)\Sigma^<_\xi(t_2,t) \\ &+ \Sigma^<_\zeta(t',t_1)G^a_{\eta\sigma}(t_1,t_2)\Sigma^a_\xi(t_2,t) \\ &+ \Sigma^r_\zeta(t',t_1)G^<_{\eta\sigma}(t_1,t_2)\Sigma^a_\xi(t_2,t)] \\ &- [\Sigma^r_\xi(t,t_1)G^r_{\sigma'\lambda}(t_1,t_2)\Sigma^>_\zeta(t_2,t') \\ &+ \Sigma^>_\xi(t,t_1)G^a_{\sigma'\lambda}(t_1,t_2)\Sigma^a_\zeta(t_2,t') \\ &+ \Sigma^r_\xi(t,t_1)G^>_{\sigma'\lambda}(t_1,t_2)\Sigma^a_\zeta(t_2,t')]G^<_{\eta\sigma}(t',t)\} \\ &- \delta_{\xi\zeta}[\delta_{\eta\sigma}G^>_{\sigma'\lambda}(t,t')\Sigma^<_\xi(t',t) \\ &+ \delta_{\sigma'\lambda}\Sigma^>_\xi(t,t')G^<_{\eta\sigma}(t',t)]. \end{aligned} \tag{20}$$

Using Fourier transformations of the central-region Green's functions and self-energies in the wide-band limit, the correlations given by Eq. (20) can be further simplified. Some correlation functions are not just functions of time difference $t-t'$. Thus, similarly as in Ref. 62 we used Wigner representation assuming that in experiments fluctuations are measured on timescales much larger than the driving period $\mathcal{T}=2\pi/\omega_L$, which is the period of one molecular spin precession. The Wigner coordinates are given by $T'=(t+t')/2$ and $\tau=t-t'$, while the correlation functions are defined as

$$S_{\xi\zeta}^{\sigma\sigma',\lambda\eta}(\tau)=\frac{1}{\mathcal{T}}\int_0^{\mathcal{T}}dt\langle\delta\hat{I}_{\xi,\sigma\sigma'}(t+\tau)\delta\hat{I}_{\zeta,\lambda\eta}(t)\rangle. \quad (21)$$

The Fourier transform of $S_{\xi\zeta}^{\sigma\sigma',\lambda\eta}(\tau)$ is given by

$$S_{\xi\zeta}^{\sigma\sigma',\lambda\eta}(\Omega,\Omega')=2\pi\delta(\Omega-\Omega')S_{\xi\zeta}^{\sigma\sigma',\lambda\eta}(\Omega), \quad (22)$$

where

$$S_{\xi\zeta}^{\sigma\sigma',\lambda\eta}(\Omega)=\int d\tau e^{i\Omega\tau}S_{\xi\zeta}^{\sigma\sigma',\lambda\eta}(\tau). \quad (23)$$

For the correlations which depend only on $t-t'$, the Wigner representation is identical to the standard representation.

Finally, using Eqs. (11) and (20), the obtained formal expression for the nonsymmetrized noise of charge current[52,63] and spin currents in standard coordinates t and t' can be written as

$$\begin{aligned}
S_{\xi\zeta}^{\nu\mu}(t,t') = &-\frac{q_\nu q_\mu}{\hbar^2}\mathrm{Tr}\Big\{\int dt_1\int dt_2\\
&\times\big\{\hat{\sigma}_\nu[\hat{G}^r(t,t_1)\hat{\Sigma}_\zeta^>(t_1,t')+\hat{G}^>(t,t_1)\hat{\Sigma}_\zeta^a(t_1,t')]\\
&\times\hat{\sigma}_\mu[\hat{G}^r(t',t_2)\hat{\Sigma}_\xi^<(t_2,t)+\hat{G}^<(t',t_2)\hat{\Sigma}_\xi^a(t_2,t)]\\
&+\hat{\sigma}_\nu[\hat{\Sigma}_\xi^>(t,t_1)\hat{G}^a(t_1,t')+\hat{\Sigma}_\xi^r(t,t_1)\hat{G}^>(t_1,t')]\\
&\times\hat{\sigma}_\mu[\hat{\Sigma}_\zeta^<(t',t_2)\hat{G}^a(t_2,t)+\hat{\Sigma}_\zeta^r(t',t_2)\hat{G}^<(t_2,t)]\\
&-\hat{\sigma}_\nu\hat{G}^>(t,t')\hat{\sigma}_\mu[\hat{\Sigma}_\zeta^r(t',t_1)\hat{G}^r(t_1,t_2)\hat{\Sigma}_\xi^<(t_2,t)\\
&+\hat{\Sigma}_\zeta^<(t',t_1)\hat{G}^a(t_1,t_2)\hat{\Sigma}_\xi^a(t_2,t)\\
&+\hat{\Sigma}_\zeta^r(t',t_1)\hat{G}^<(t_1,t_2)\hat{\Sigma}_\xi^a(t_2,t)]\\
&-\hat{\sigma}_\nu[\hat{\Sigma}_\xi^r(t,t_1)\hat{G}^r(t_1,t_2)\hat{\Sigma}_\zeta^>(t_2,t')\\
&+\hat{\Sigma}_\xi^>(t,t_1)\hat{G}^a(t_1,t_2)\hat{\Sigma}_\zeta^a(t_2,t')\\
&+\hat{\Sigma}_\xi^r(t,t_1)\hat{G}^>(t_1,t_2)\hat{\Sigma}_\zeta^a(t_2,t')]\hat{\sigma}_\mu\hat{G}^<(t',t)\big\}\\
&-\delta_{\xi\zeta}\hat{\sigma}_\nu[\hat{G}^>(t,t')\hat{\sigma}_\mu\hat{\Sigma}_\xi^<(t',t)\\
&+\hat{\Sigma}_\xi^>(t,t')\hat{\sigma}_\mu\hat{G}^<(t',t)]\Big\}, \quad (24)
\end{aligned}$$

where Tr denotes the trace in the electronic spin space.

The symmetrized noise of charge and spin currents reads[1,52]

$$S_{\xi\zeta S}^{\nu\mu}(t,t')=\frac{1}{2}\langle\{\delta\hat{I}_{\xi\nu}(t),\delta\hat{I}_{\zeta\mu}(t')\}\rangle, \quad (25)$$

where $\{,\}$ denotes the anticommutator. According to Eqs. (11), (21), (23) and (25), in the Wigner representation the nonsymmetrized noise spectrum reads

$$\begin{aligned}
S_{\xi\zeta}^{\nu\mu}(\Omega) &= \int d\tau e^{i\Omega\tau}S_{\xi\zeta}^{\nu\mu}(\tau)\\
&= \int d\tau e^{i\Omega\tau}\frac{1}{\mathcal{T}}\int_0^{\mathcal{T}}dt\langle\delta\hat{I}_{\xi\nu}(t+\tau)\delta\hat{I}_{\zeta\mu}(t)\rangle\\
&= -\frac{q_\nu q_\mu}{\hbar^2}\sum_{\sigma\sigma'}\sum_{\lambda\eta}(\sigma_\nu)_{\sigma\sigma'}(\sigma_\mu)_{\lambda\eta}S_{\xi\zeta}^{\sigma\sigma',\lambda\eta}(\Omega), \quad (26)
\end{aligned}$$

while the symmetrized noise spectrum equals

$$\begin{aligned}
S_{\xi\zeta S}^{\nu\mu}(\Omega) &= \frac{1}{2}[S_{\xi\zeta}^{\nu\mu}(\Omega)+S_{\zeta\xi}^{\mu\nu}(-\Omega)]\\
&= -\frac{q_\nu q_\mu}{2\hbar^2}\sum_{\sigma\sigma'}\sum_{\lambda\eta}(\sigma_\nu)_{\sigma\sigma'}(\sigma_\mu)_{\lambda\eta}S_{\xi\zeta S}^{\sigma\sigma',\lambda\eta}(\Omega),
\end{aligned} \quad (27)$$

where $S_{\xi\zeta S}^{\sigma\sigma',\lambda\eta}(\Omega)=[S_{\xi\zeta}^{\sigma\sigma',\lambda\eta}(\Omega)+S_{\zeta\xi}^{\lambda\eta,\sigma\sigma'}(-\Omega)]/2$. It is of experimental interest to investigate zero-frequency noise power.

III. SHOT NOISE OF CHARGE CURRENT

For the charge current noise it is convenient to drop superscripts $\nu=\mu=0$. The charge current noise spectrum can be obtained as[39]

$$S_{\xi\zeta}(\Omega)=-\frac{e^2}{\hbar^2}[S_{\xi\zeta}^{11,11}+S_{\xi\zeta}^{11,22}+S_{\xi\zeta}^{22,11}+S_{\xi\zeta}^{22,22}](\Omega). \quad (28)$$

In this section we analyze the zero-frequency noise power of the charge current $S_{\xi\zeta}=S_{\xi\zeta}(0)$ at zero temperature. Taking into account that thermal noise disappears at zero temperature, the only contribution to the charge current noise comes from the shot noise. The tunnel couplings between the molecular orbital and the leads $\Gamma_\xi(\epsilon)=2\pi\sum_k|V_{k\xi}|^2\delta(\epsilon-\epsilon_{k\xi})$ are considered symmetric and in the wide band limit $\Gamma_L=\Gamma_R=\Gamma/2$.

The charge current from lead ξ can be expressed as

$$\begin{aligned}
I_\xi = &\frac{e\Gamma_\xi\Gamma_\zeta}{\hbar}\int\frac{d\epsilon}{2\pi}[f_\xi(\epsilon)-f_\zeta(\epsilon)]\\
&\times\sum_{\substack{\sigma\sigma'\\ \sigma\neq\sigma'}}\frac{|G_{\sigma\sigma}^{0r}(\epsilon)|^2[1+\gamma^2|G_{\sigma'\sigma'}^{0r}(\epsilon+\sigma'\omega_L)|^2]}{|1-\gamma^2G_{\sigma\sigma}^{0r}(\epsilon)G_{\sigma'\sigma'}^{0r}(\epsilon+\sigma'\omega_L)|^2}, \quad (29)
\end{aligned}$$

where $\xi\neq\zeta$, while $G_{\sigma\sigma}^{0r}(\epsilon)$ are matrix elements of $\hat{G}^{0r}(\epsilon)=[\epsilon-\epsilon_0+i\sum_\xi\Gamma_\xi/2-\hat{\sigma}_z(g\mu_BB+JS_z)/2]^{-1}$.[64,65] The conservation of the charge current implies that $S_{LL}(0)+S_{LR}(0)=0$. Thus, it is sufficient to study only one correlation function.

Tunning the parameters in the system such as the bias voltage $eV=\mu_L-\mu_R$, where μ_L and μ_R are the chemical potentials of the leads, $\vec{B}$ and the tilt angle θ, the shot noise can be controlled and minimized.

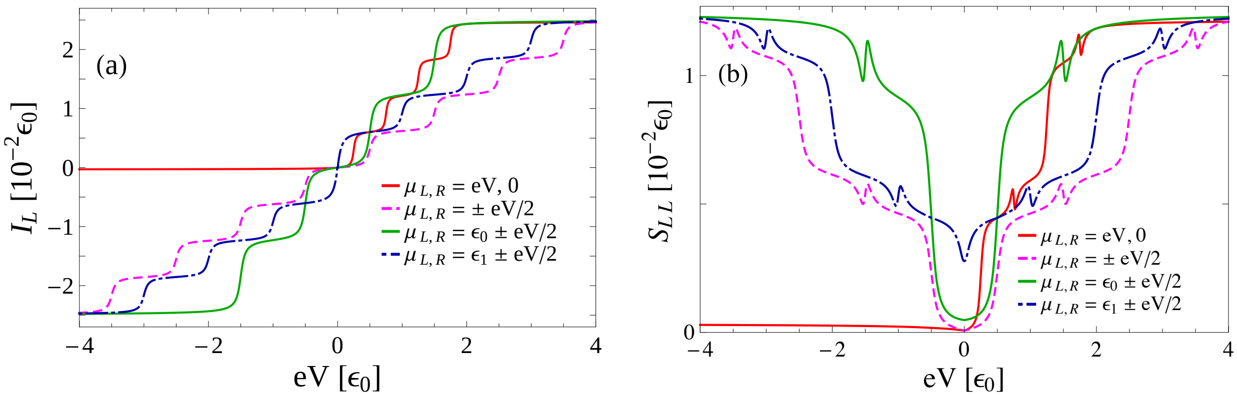

FIG. 2. (Color online) (a) Charge current I_L and (b) auto-correlation shot noise S_{LL} as functions of bias-voltage eV. All plots are obtained at zero temperature, with $\vec{B} = B\vec{e}_z$. The other parameters are: $\Gamma_L = \Gamma_R = \Gamma/2$, $\Gamma = 0.05\,\epsilon_0$, $\omega_L = 0.5\,\epsilon_0$, $J = 0.01\,\epsilon_0$, $S = 100$, and $\theta = \pi/2$. The molecular quasienergy levels are located at: $\epsilon_1 = 0.25\,\epsilon_0$, $\epsilon_2 = 0.75\,\epsilon_0$, $\epsilon_3 = 1.25\,\epsilon_0$, and $\epsilon_4 = 1.75\,\epsilon_0$.

In Fig. 2(a) we present the average charge current as a staircase function of bias voltage, where the bias is varied in four different ways. In the presence of the external magnetic field and the precessing molecular spin, the initially degenerate electronic level with energy ϵ_0 results in four nondegenerate transport channels, which has an important influence on the noise. Each step corresponds to a new available transport channel. The transport channels are located at the Floquet quasienergies[55] $\epsilon_1 = \epsilon_0 - (\omega_L/2) - (JS/2)$, $\epsilon_2 = \epsilon_0 + (\omega_L/2) - (JS/2)$, $\epsilon_3 = \epsilon_0 - (\omega_L/2) + (JS/2)$, and $\epsilon_4 = \epsilon_0 + (\omega_L/2) + (JS/2)$, which are calculated using the Floquet theorem.[20,66–69]

The correlated current fluctuations give nonzero noise power, which is presented in Fig. 2(b). The noise power shows the molecular quasienergy spectrum and each step or dip-like feature in the noise denotes the energy of a new available transport channel. The noise has two steps and two dip-like features which correspond to these resonances. Charge current and noise power are saturated for large bias voltages. If the Fermi levels of the leads lie below the resonances, the shot noise approaches zero for $eV \to 0$ [red and dashed pink lines in Fig. 2(b)]. This is due to the fact that a small number of electron states can participate in transport inside this small bias window and both current and noise are close to 0. If the bias voltage is varied with respect to the resonant energy ϵ_1 such that $\mu_{L,R} = \epsilon_1 \pm eV/2$ [dot-dashed blue line in Fig. 2(b)], or with respect to ϵ_0 such that $\mu_{L,R} = \epsilon_0 \pm eV/2$ [green line in Fig. 2(b)], we observe a valley at zero bias, which corresponds to $\mu_L = \mu_R = \epsilon_1$ in the first case, and nonzero noise in the second case. As $eV = 0$ the net tunneling current is zero, but the precession-assisted inelastic processes, involving absorption of an energy quantum ω_L give rise to the noise here.

Thus, for $eV \to 0$ the Fano factor $F \gg 1$, indicating that the noise is super Poissonian, as depicted in Fig. 3. Due to the absorption (emission) processes[20] and quantum interference effect the Fano factor is a deformed step-like function, where each step corresponds to a resonance. As the bias voltage is increased, the noise is enhanced since the number of the correlated electron pairs increases with the increase of the Fermi level. For larger bias, due to the absorption and emission of an energy quantum ω_L, electrons can jump to a level with higher energy or lower level during the transport, and the Fano factor $F < 1$ indicating the sub-Poissonian noise. Around resonances $\mu_{L,R} = \epsilon_i$, $i = 1, 2, 3, 4$, the probability of transmission is very high, resulting in the small Fano factor. Elastic tunneling contributes to the sub-Poissonian Fano factor around resonances and competes with the spin-flip events caused by the molecular spin precession. However, if the resonant quasienergy levels are much higher than the Fermi energy of the leads, the probability of transmission is very low and the Fano factor is close to 1 as shown in Fig. 3 (red line). This means that the stochastic processes are uncorrelated. If the two levels connected with the inelastic photon emission (absorption) tunnel processes, or all four levels, lie between the Fermi levels of the leads, the Fano factor approaches 1/2, which is in agreement with Ref. 70. For $eV = \epsilon_3$ [see Fig. 3 (red line)] a spin down electron can tunnel elastically, or inelastically in a spin-flip process leading to the increase of the Fano factor. Spin-flip processes increase electron traveling time, leading to sub-Poissonian noise. Pauli exclusion principle also leads to sub-Poissonian noise, since it prevents the double occupancy of a level.

The precessing molecular spin induces quantum interference between the transport channels connected with spin-flip events and the change of energy by one energy quantum ω_L, i.e., between levels with energies ϵ_1 and $\epsilon_2 = \epsilon_1 + \omega_L$, or ϵ_3 and $\epsilon_4 = \epsilon_3 + \omega_L$. The destructive quantum interference effects manifest themselves in the form of dip-like features in Fig. 2(b). When one or both pairs of the levels connected with spin-flip events enter the bias-voltage window, then an electron from the left lead can tunnel through both levels via elastic or inelas-

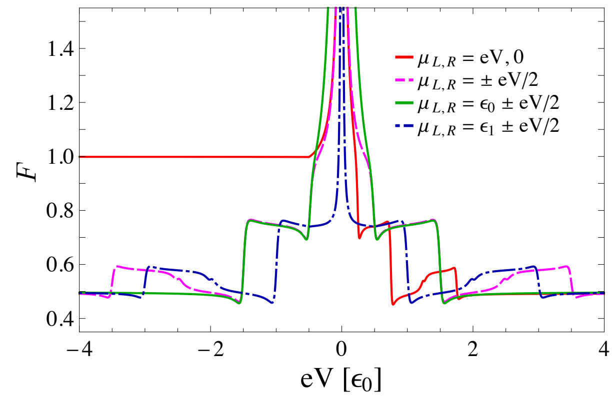

FIG. 3. (Color online) Fano factor F as a function of bias-voltage eV. All plots are obtained at zero temperature, with $\vec{B} = B\vec{e}_z$. The other parameters are set to: $\Gamma = 0.05\,\epsilon_0$, $\Gamma_L = \Gamma_R = \Gamma/2$, $\omega_L = 0.5\,\epsilon_0$, $J = 0.01\,\epsilon_0$, $S = 100$, and $\theta = \pi/2$. The positions of the molecular quasienergy levels are: $\epsilon_1 = 0.25\,\epsilon_0$, $\epsilon_2 = 0.75\,\epsilon_0$, $\epsilon_3 = 1.25\,\epsilon_0$, and $\epsilon_4 = 1.75\,\epsilon_0$.

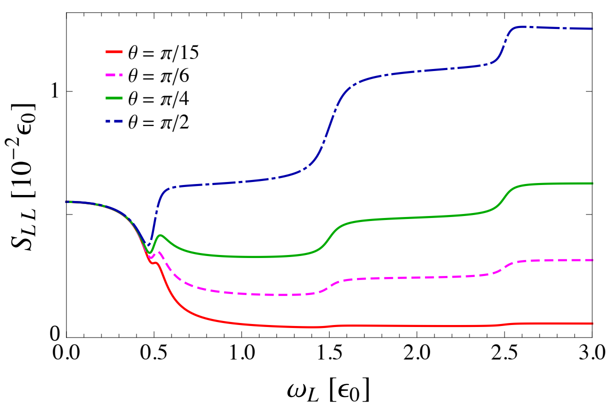

FIG. 4. (Color online) Shot noise of charge current S_{LL} as a function of the Larmor frequency ω_L, for different tilt angles θ, with $\vec{B} = B\vec{e}_z$, at zero temperature. The other parameters are: $\Gamma = 0.05\,\epsilon_0$, $\Gamma_L = \Gamma_R = \Gamma/2$, $\mu_L = 0.75\,\epsilon_0$, $\mu_R = 0.25\,\epsilon_0$, $J = 0.01\,\epsilon_0$, and $S = 100$. For $\omega_L = \mu_L - \mu_R$ we observe a dip due to destructive quantum interference.

tic spin-flip processes. Different tunneling pathways ending in the final state with the same energy, destructively interfere, similarly as in the Fano effect.[15] Namely, the state with lower energy, ϵ_1 (or ϵ_3) mimics the discrete state in the Fano effect. An electron tunnels into the state ϵ_1 (or ϵ_3), undergoes a spin-flip and absorbs an energy quantum ω_L. The other state with energy ϵ_2 (or ϵ_4) is an analog of the continuum in the Fano effect, and the electron tunnels elastically through this level. These two tunneling processes, one elastic and the other inelastic interfere, leading to a dip-like feature in the noise power. If we vary, for instance, the bias-voltage as $eV = \mu_L$, where $\mu_R = 0$ [Fig. 2(b), red line], we observe dip-like features for $eV = \epsilon_2$ and $eV = \epsilon_4$. The destructive interference effect is also presented in Fig. 4, where noise

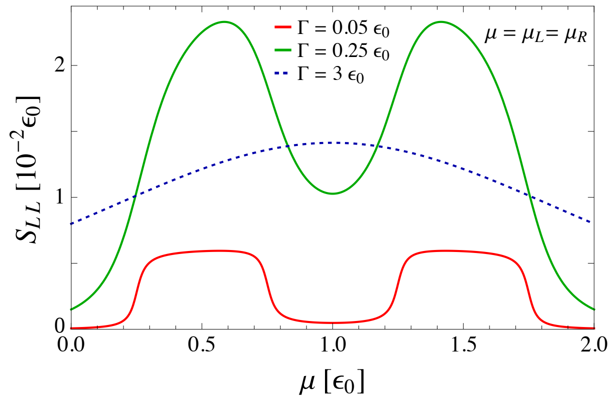

FIG. 5. (Color online) Shot noise of charge current S_{LL} as a function of the chemical potential of the leads $\mu = \mu_L = \mu_R$, with $\vec{B} = B\vec{e}_z$, for three different couplings Γ, where $\Gamma_L = \Gamma_R = \Gamma/2$, at zero temperature. The other parameters are: $\omega_L = 0.5\,\epsilon_0$, $J = 0.01\,\epsilon_0$, $S = 100$, and $\theta = \pi/2$. The molecular quasienergy levels are positioned at: $\epsilon_1 = 0.25\,\epsilon_0$, $\epsilon_2 = 0.75\,\epsilon_0$, $\epsilon_3 = 1.25\,\epsilon_0$, and $\epsilon_4 = 1.75\,\epsilon_0$.

power S_{LL} is depicted as a function of ω_L. Here, we observe a dip due to the quantum interference effect around $\omega_L = 0.5\,\epsilon_0$, which corresponds to $\mu_L = \epsilon_2$ and $\mu_R = \epsilon_1$. The other two steps in Fig. 4 occur when the Fermi energy of the right or left lead is in resonance with one of the quasienergy levels. The magnitude of the precessing component of the molecular spin, which induces spin-flip processes between molecular quasienergy levels, equals $JS\sin(\theta)/2$. Therefore, the dip increases with the increase of the tilt angle θ, and is maximal and distinct for $\theta = \pi/2$.

Finally, in Fig. 5 we plotted the noise power of charge current S_{LL} as a function of $\mu = \mu_L = \mu_R$ at zero temperature. It shows nonmonotonic dependence on the tunneling rates Γ. For small Γ (Fig. 5, red line) the noise is increased if μ is positioned between levels connected with spin-flip events, and is contributed only by absorption processes of an energy quantum ω_L, as we vary the chemical potentials. For larger Γ (Fig. 5, green line), the charge current noise is increased since levels broaden and overlap, and more electrons can tunnel. With further increase of Γ (Fig. 5, dotted blue line) the noise starts to decrease, and it is finally suppressed for $\Gamma \gg \omega_L$, since a current-carrying electron sees the molecular spin as nearly static in this case, leading to the reduction of the inelastic spin-flip processes.

IV. SHOT NOISE OF SPIN CURRENT AND SPIN-TRANSFER TORQUE

In this section we present the spin-current noise-spectrum components and relations between them. Later we introduce the noise of spin-transfer torque and investigate the zero-frequency spin-torque shot noise at zero temperature. The components of the nonsymmetrized spin-current noise spectrum read

$$S^{xx}_{\xi\zeta}(\Omega) = -\frac{1}{4}[S^{12,21}_{\xi\zeta} + S^{21,12}_{\xi\zeta}](\Omega), \tag{30}$$

$$S^{xy}_{\xi\zeta}(\Omega) = -\frac{i}{4}[S^{12,21}_{\xi\zeta} - S^{21,12}_{\xi\zeta}](\Omega), \tag{31}$$

$$S^{zz}_{\xi\zeta}(\Omega) = -\frac{1}{4}[S^{11,11}_{\xi\zeta} - S^{11,22}_{\xi\zeta} - S^{22,11}_{\xi\zeta} + S^{22,22}_{\xi\zeta}](\Omega), \tag{32}$$

where Eq. (32) denotes the noise of the z component of the spin current.[37,39] Since the polarization of the spin current precesses in the xy plane, the remaining components of the spin-current noise spectrum satisfy the following relations:

$$S^{yy}_{\xi\zeta}(\Omega) = S^{xx}_{\xi\zeta}(\Omega), \tag{33}$$

$$S^{yx}_{\xi\zeta}(\Omega) = -S^{xy}_{\xi\zeta}(\Omega), \tag{34}$$

$$S^{xz}_{\xi\zeta}(\Omega) = S^{zx}_{\xi\zeta}(\Omega) = S^{yz}_{\xi\zeta}(\Omega) = S^{zy}_{\xi\zeta}(\Omega) = 0. \tag{35}$$

Taking into account that the spin current is not a conserved quantity, it is important to notice that the complete information from the noise spectrum can be obtained by studying both auto-correlation noise spectrum $S^{jk}_{\xi\xi}(\Omega)$ and cross-correlation noise spectrum $S^{jk}_{\xi\zeta}(\Omega)$, $\zeta \neq \xi$. Therefore, it is more convenient to investigate the spin-torque noise spectrum, where both auto-correlation and cross-correlation noise components of spin currents are included. The spin-transfer torque operator can be defined as

$$\hat{T}_j = -(\hat{I}_{Lj} + \hat{I}_{Rj}), \qquad j = x, y, z; \tag{36}$$

while its fluctuation reads

$$\delta\hat{T}_j(t) = -[\delta\hat{I}_{Lj}(t) + \delta\hat{I}_{Rj}(t)]. \tag{37}$$

Accordingly, the nonsymmetrized and symmetrized spin-torque noise can be obtained using the spin-current noise components as

$$S^{jk}_T(t,t') = \langle\delta\hat{T}_j(t)\delta\hat{T}_k(t')\rangle = \sum_{\xi\zeta} S^{jk}_{\xi\zeta}(t,t'), \qquad j,k = x,y,z; \tag{38}$$

$$S^{jk}_{TS}(t,t') = \frac{1}{2}[S^{jk}_T(t,t') + S^{kj}_T(t',t)], \tag{39}$$

with the corresponding noise spectrums given by

$$S^{jk}_T(\Omega) = \sum_{\xi\zeta} S^{jk}_{\xi\zeta}(\Omega), \tag{40}$$

$$S^{jk}_{TS}(\Omega) = \sum_{\xi\zeta} S^{jk}_{\xi\zeta S}(\Omega). \tag{41}$$

According to Eqs. (33), (34), and (40), $S^{xx}_T(\Omega) = S^{yy}_T(\Omega)$ and $S^{yx}_T(\Omega) = -S^{xy}_T(\Omega)$.

In the remainder of the section we investigate the zero-frequency spin-torque shot noise $S^{jk}_T = S^{jk}_T(0)$ at zero temperature, where $S^{xx}_T(0) = S^{xx}_{TS}(0)$, $S^{yy}_T(0) = S^{yy}_{TS}(0)$, $S^{zz}_T(0) = S^{zz}_{TS}(0)$, while $S^{xy}_T(0)$ is a complex imaginary function, and $S^{xy}_{TS}(0) = 0$ according to Eqs. (34) and (41). Since $S^{xx}_T(0) = S^{yy}_T(0)$, all results and discussions related to $S^{xx}_T(0)$ also refer to $S^{yy}_T(0)$.

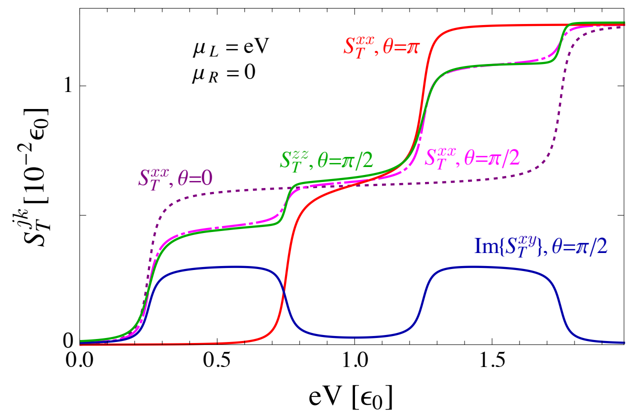

FIG. 6. (Color online) Spin-torque shot noise components S^{jk}_T as functions of the bias voltage eV for $\mu_R = 0$, $\mu_L = eV$. All plots are obtained at zero temperature, with $\vec{B} = B\vec{e}_z$, and $\Gamma_L = \Gamma_R = \Gamma/2$, for $\Gamma = 0.05\,\epsilon_0$. The other parameters are set to: $\omega_L = 0.5\,\epsilon_0$, $J = 0.01\,\epsilon_0$, and $S = 100$. The molecular quasienergy levels lie at: $\epsilon_1 = 0.25\,\epsilon_0$, $\epsilon_2 = 0.75\,\epsilon_0$, $\epsilon_3 = 1.25\,\epsilon_0$, and $\epsilon_4 = 1.75\,\epsilon_0$.

Spin currents $I_{\xi x}$ and $I_{\xi y}$ are periodic functions of time, with period $\mathcal{T} = 2\pi/\omega_L$, while $I_{\xi z}$ is time-independent. It has already been demonstrated that spin-flip processes contribute to the noise of spin current.[37] The presence of the precessing molecular spin affects the spin current noise. Since the number of particles with different spins changes due to spin-flip processes, additional spin-current fluctuations are generated. Currents with the same and with different spin orientations are correlated during transport. Due to the precessional motion of the molecular spin, inelastic spin currents with spin-flip events induce noise of spin currents and spin-torque noise, which can be nonzero even for $eV = 0$. The noise component S^{xy}_T is induced by the molecular spin precession and vanishes for a static molecular spin. The noises of spin currents and spin-transfer torque are driven by the bias voltage and by the molecular spin precession. Hence, in the case when both the molecular spin is static (absence of inelastic spin-flip processes) and $eV = 0$ (no net contribution of elastic tunneling processes), they are all equal to zero. The noise of spin-transfer torque can be modified by adjusting system parameters such as the bias-voltage eV, the magnetic field $\vec{B}$, or the tilt angle θ.

In Fig. 6 we present zero-frequency spin-torque noise components $S^{xx}_T = S^{yy}_T$, $\mathrm{Im}\{S^{xy}_T\}$, and S^{zz}_T as functions of the bias voltage $eV = \mu_L - \mu_R$, for $\mu_R = 0$ and different tilt angles θ between $\vec{B}$ and $\vec{S}$, at zero temperature. They give information on available transport channels and inelastic spin-flip processes. The magnitude of the torque noise at resonance energies ϵ_i, $i = 1, 2, 3, 4$, is determined by θ. In cases $\theta = 0$ and $\theta = \pi$, there are only two transport channels of opposite spins determined by the resulting Zeeman field $B \pm JS/g\mu_B$. The component S_T^{xx} shows two steps with equal heights located at these resonances, where the only contribution to the spin-torque noise comes from elastic tunneling events (dotted purple and red lines in Fig. 6). For $\theta = \pi/2$, the elastic tunneling contributes with four steps with equal heights located at resonances ϵ_i, but due to the contributions of the inelastic precession-assisted processes between quasienergy levels $\epsilon_1(\epsilon_3)$ and $\epsilon_2(\epsilon_4)$, the heights of the steps in S_T^{xx} are not equal anymore (dot-dashed pink line in Fig. 6). Here, we observed that the contribution of the inelastic tunneling processes to S_T^{xx}, involving absorption of an energy quantum ω_L and a spin-flip, shows steps at spin-down quasienergy levels ϵ_1 and ϵ_3, while it is constant between and after the bias has passed these levels. The component S_T^{zz} shows similar behavior (green line in Fig. 6). Similarly as in the case of the inelastic tunneling involving the absorption of one energy quantum ω_L, in $S_T^{xx} = S_T^{yy}$ we observed inelastic spin-flip processes involving the absorption of two energy quanta $2\omega_L$, in the form of steps at spin-down levels ϵ_1, ϵ_3, $\epsilon_2 - 2\omega_L$ and $\epsilon_4 - 2\omega_L$, which have negligible contribution compared to the other terms. These processes are a result of correlations of two oscillating spin-currents. For large bias voltage the spin-torque noise components S_T^{xx} and S_T^{zz} become saturated.

The behavior of the component $\mathrm{Im}\{S_T^{xy}\}$ is completely different in nature. It is contributed only by one energy quantum ω_L absorption (emission) spin-flip processes. Interestingly, we obtained the following relation between the Gilbert damping parameter α,[54,55] and $\mathrm{Im}\{S_T^{xy}\}$, at arbitrary temperature

$$\mathrm{Im}\{S_T^{xy}\} = \frac{\omega_L S \sin^2(\theta)}{2}\alpha. \quad (42)$$

Hence, the component $\mathrm{Im}\{S_T^{xy}\}$ is increased for Fermi levels of the leads positioned in the regions where inelastic tunneling processes occur (blue line in Fig. 6).

The spin-torque noise is influenced by the magnetic field $\vec{B}$, since it determines the spin-up and spin-down molecular quasienergy levels. The dependence of S_T^{xx}, $\mathrm{Im}\{S_T^{xy}\}$, and S_T^{zz} on the Larmor frequency ω_L is depicted in Fig. 7. The steps, dips or peaks in the plots are located at resonant tunneling frequencies $\omega_L = \pm|2\mu_{L,R} - 2\epsilon_0 \pm JS|$. For $\omega_L = 0$ there are only two transport channels, one at energy $\epsilon_0 + JS/2$ which is equal to the Fermi energy of the left lead, and the other at $\epsilon_0 - JS/2$ located between μ_L and μ_R. The contributions of the elastic spin transport processes through these levels result in dips in the components S_T^{xx} and S_T^{zz}, while $\mathrm{Im}\{S_T^{xy}\} = 0$. For $\omega = \epsilon_0$ corresponding to $\mu_R = \epsilon_1$ and $\mu_R = \epsilon_4 - 2\omega_L$, both the elastic and spin-flip tunneling events involving the absorption of energy of one quantum ω_L contribute with a dip, while the spin-flip processes involving the absorption of an energy equal to

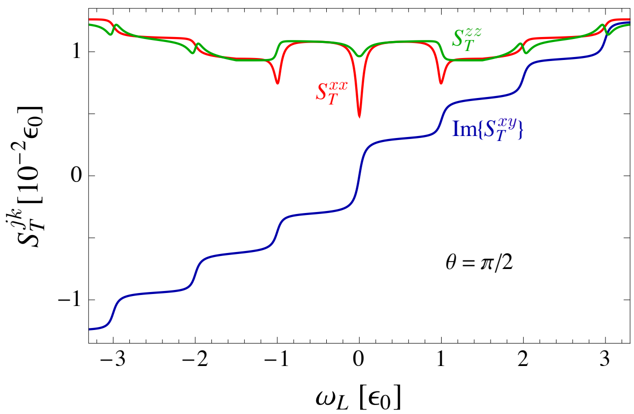

FIG. 7. (Color online) Spin-torque shot noise components S_T^{jk} as functions of the Larmor frequency ω_L for $\theta = \pi/2$, $\mu_R = 0$, and $\mu_L = 1.5\,\epsilon_0$. All plots are obtained for $\vec{B} = B\vec{e}_z$ at zero temperature. The other parameters are: $\Gamma_L = \Gamma_R = \Gamma/2$, $\Gamma = 0.05\,\epsilon_0$, $J = 0.01\,\epsilon_0$, and $S = 100$.

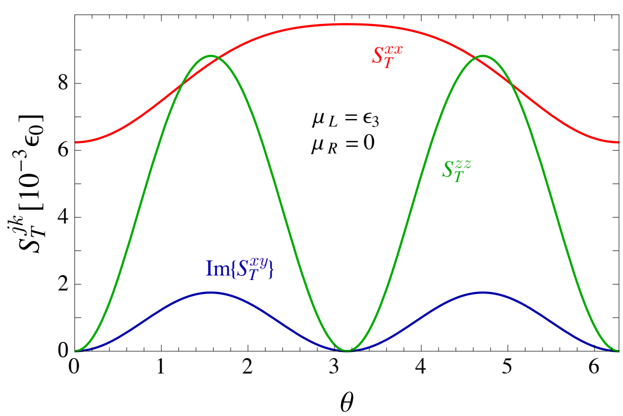

FIG. 8. (Color online) Spin-torque shot noise components as functions of the tilt angle θ for $\mu_L = \epsilon_3$, $\mu_R = 0$. All plots are obtained at zero temperature, with $\vec{B} = B\vec{e}_z$, $\Gamma = 0.05\,\epsilon_0$, and $\Gamma_L = \Gamma_R = \Gamma/2$. The other parameters are: $\omega_L = 0.5\,\epsilon_0$, $J = 0.01\,\epsilon_0$, and $S = 100$.

$2\omega_L$ contribute with a peak to the component S_T^{xx}. For $\omega_L = 2\,\epsilon_0$ and $\omega_L = 3\,\epsilon_0$ corresponding to $\mu_L = \epsilon_2$ and $\mu_R = \epsilon_3$, both elastic and spin-flip processes with the absorption of an energy equal to ω_L contribute with a step, while the inelastic processes involving the absorption of an energy $2\omega_L$ give negligible contribution to S_T^{xx}. The component S_T^{zz} shows dips at these two points, since here the dominant contribution comes from inelastic tunneling spin-flip events. The component S_T^{zz} is an even, while $\mathrm{Im}\{S_T^{xy}\}$ is an odd function of ω_L. The spin-torque noise S_T^{xx} is an even function of ω_L for $\theta = \pi/2$.

The spin-torque noise components as functions of θ for $\mu_L = \epsilon_3$ and $\mu_R = 0$ at zero temperature are shown in Fig. 8. The magnitudes and the appearance of the spin-torque noise components at resonance energies ϵ_i can be controlled by θ, since it influences the polarization of the spin current. Here we see that both S_T^{zz} and $\mathrm{Im}\{S_T^{xy}\}$ are zero for $\theta = 0$ and $\theta = \pi$, as the molecular spin is static and its magnitude is constant along z-direction in both cases. These torque-noise components take their maximum values for $\theta = \pi/2$, where both elastic and inelastic tunneling contributions are maximal. The component S_T^{xx} takes its minimum value for $\theta = 0$, and its maximum value for $\theta = \pi$, with only elastic tunneling contributions in both cases. For $\theta = \pi/2$ the inelastic tunneling events give maximal contribution, while energy conserving processes give minimal contribution to S_T^{xx}.

V. CONCLUSIONS

In this article we have first theoretically studied noise of charge and spin transport through a small junction, consisting of a single molecular orbital in the presence of a molecular spin precessing with Larmor frequency ω_L in a constant magnetic field. The orbital is connected to two Fermi leads. We used the Keldysh nonequilibrium Green's functions method to derive the noise components of charge and spin currents and spin-transfer torque.

Then we analyzed the shot noise of charge current and observed characteristics which differ from the ones in the current. In the noise power we observed dip-like features which we attribute to inelastic processes, due to the molecular spin precession, leading to the quantum interference effect between correlated transport channels.

Since the inelastic tunneling processes lead to a spin-transfer torque acting on the molecular spin, we have also investigated the spin-torque noise components contributed by these processes, involving the change of energy by an energy quantum ω_L. The spin-torque noise components are driven by both the bias voltage and the molecular spin precession. The in-plane noise components S_T^{xx} and S_T^{yy} are also contributed by the processes involving the absorption of an energy equal to $2\omega_L$. We obtained the relation between $\mathrm{Im}\{S_T^{xy}\}$ and the Gilbert damping coefficient α at arbitrary temperature.

Taking into account that the noise of charge and spin transport can be controlled by the parameters such as bias voltage and external magnetic field, our results might be useful in molecular electronics and spintronics. Finding a way to control the spin states of single-molecule magnets in tunnel junctions could be one of the future tasks.

ACKNOWLEDGMENTS

We would like to thank Fei Xu for useful discussions. We gratefully acknowledge the financial support from the Deutsche Forschungsgemeinschaft through the SFB 767 *Controlled Nanosystems* and an ERC Advanced Grant *UltraPhase* of Alfred Leitenstorfer.

1. Y. M. Blanter and M. Büttiker, Physics Reports, **336**, 2 (2000).
2. W. Schottky, Ann. Phys. (Leipzig) **57**, 541 (1918).
3. M. Büttiker, Phys. Rev. Lett. **65**, 2901 (1990).
4. A. Kumar, L. Saminadayar, D. C. Glattli, Y. Jin, and B. Etienne, Phys. Rev. Lett. **76**, 2778 (1996).
5. V. V. Kuznetsov, E. E. Mendez, X. Zuo, G. L. Snider, and E. T. Croke, Phys. Rev. Lett. **85**, 397 (2000).
6. O. M. Bulashenko and J. M. Rubí, Phys. Rev. B **64**, 045307 (2001).
7. O. M. Bulashenko and J. M. Rubí, Phys. Rev. B **67**, 115322 (2003).
8. E. Onac, F. Balestro, B. Trauzettel, C. F. J. Lodewijk, and L. P. Kouwenhoven, Phys. Rev. Lett. **96**, 026803 (2006).
9. A. E. Miroschnichenko, S. Flach, and Y. S. Kivshar, Rev. Mod. Phys. **82**, 2257 (2010).
10. C. M. Guédon, H. Valkenier, T. Markussen, K. S. Thygesen, J. C. Hummelen, and S. J. van der Molen, Nature Nanotech. **7**, 305 (2012).
11. H. Vázquez, R. Skouta, S. Schneebeli, M. Kamenetska, R. Beslov, L. Venkataraman, and M. S. Hybertsen, Nature Nanotech. **7**, 663 (2012).
12. R. Stadler, Phys. Rev. B **80**, 125401 (2009).
13. M. A. Ratner, J. Phys. Chem. **94**, 4877 (1990).
14. T. Hansen, G. C. Solomon, D. Q. Andrews, and M. A. Ratner, J. Chem. Phys. **131**, 194704 (2009).
15. U. Fano, Phys. Rev. **124**, 1866 (1961).
16. J. Faist, F. Capasso, C. Sirtori, K. W. West, and L. N. Pfeiffer, Nature **390**, 589 (1997).
17. O. Entin-Wohlman, Y. Imry, S. A. Gurvitz, and A. Aharony, Phys. Rev. B **75**, 193308 (2007).
18. D. Sánchez and L. Serra, Phys. Rev. B **74**, 153313 (2006).
19. Piotr Stefański, J. Phys.: Cond. Matter **22**, 505303 (2010).
20. B. H. Wu and C. Timm, Phys. Rev. B **81**, 075309 (2010).
21. S. A. Gurvitz, D. Mozyrsky, and G. P. Berman, Phys. Rev. B **72**, 205341 (2005).
22. S. A. Gurvitz, IEEE Trans. Nanotechnology **4**, 45 (2005).
23. D. Mozyrsky, L. Fedichkin, S. A. Gurvitz, and G. P. Berman, Phys. Rev. B **66**, 161313 (2002).
24. E. G. Mishchenko, Phys. Rev. B **68**, 100409(R) (2003).
25. F. M. Souza, A. P. Jauho, and J. C. Egues, Phys. Rev. B **78**, 155303 (2008).
26. T. Gramespacher and M. Büttiker, Phys. Rev. Lett. **81**, 2763 (1998).
27. R. Landauer, Nature **392**, 658 (1998).
28. M. Büttiker, Phys. Rev. B **46**, 12485 (1992).
29. O. L. Bø and Y. Galperin, J. Phys.: Condens. Matter **8** 3033 (1996).
30. B. Dong and X. L. Lei, J. Phys.: Condens. Matter **14**, 4963 (2002).
31. M. Galperin, A. Nitzan, and M. A. Ratner, Phys. Rev. B **74**, 075326 (2006).
32. G.-H. Ding and T.-K. Ng, Phys. Rev. B **56**, 15521 (1997).
33. X. Y. Shen, B. Dong, X. L. Lei, N. J. M. Horing, Phys. Rev. B **76**, 115308 (2007).
34. S. Kohler, J. Lehmann, and P. Hänggi, Phys. Rep. **406**, 379 (2005).
35. A. Lamacraft, Phys. Rev. B **69**, 081301(R) (2004).

[36] M. Zareyan and W. Belzig, Europhys. Lett. **70**, 817 (2005).
[37] B. Wang, J. Wang, and H. Guo, Phys. Rev. B **69**, 153301 (2004).
[38] S. H. Ouyang, C. H. Lam, and J. Q. You, Euro. Phys. J. B **64**, 67 (2008).
[39] O. Sauret and D. Feinberg, Phys. Rev. Lett. **92**, 106601 (2004).
[40] M. J. Stevens, A. L. Smirl, R. D. R. Bhat, A. Najmale, J. E. Sipe, and H. M. van Driel, Phys. Rev. Lett. **90**, 136603 (2003).
[41] A. Brataas, Y. Tserkovnyak, G. E. W. Bauer, and B. I. Halperin, Phys. Rev. B **66**, 060404(R) (2002).
[42] R. L. Dragomirova and B. K. Nikolić, Phys. Rev. B **75**, 085328 (2007).
[43] Y. He, D. Hou, and R. Han, J. Appl. Phys. **101**, 023710 (2007).
[44] Y. Yu, H. Zhan, L. Wan, B. Wang, Y. Wei, Q. Sun and J. Wang, Nanotechnology **24**, 155202 (2013).
[45] J. Foros, A. Brataas, Y. Tserkovnyak, and G. E. W. Bauer, Phys. Rev. Lett. **95**, 016601 (2005).
[46] A. L. Chudnovskiy, J. Swiebodzinski, and A. Kamenev, Phys. Rev. Lett. **101**, 066601 (2008).
[47] Y. Wang and L. J. Sham, Phys. Rev. B **85**, 092403 (2012).
[48] Y. Wang and L. J. Sham, Phys. Rev. B **87**, 174433 (2013).
[49] J.C. Slonczewski, J. Magn. Magn. Mater. **159**, L1 (1996).
[50] L. Berger, Phys. Rev. B **54**, 9353 (1996).
[51] A.-P.Jauho, N. S. Wingreen, and Y. Meir, Phys. Rev. B **50**, 5528 (1994).
[52] A.-P. Jauho and H. Haug, *Quantum Kinetics in Transport and Optics of Semiconductors* (Springer, Berlin, 2008).
[53] N. S. Wingreen, A.-P.Jauho, and Y. Meir, Phys. Rev. B **48**, 8487 (1993).
[54] M. Filipović, C. Holmqvist, F. Haupt, and W. Belzig, Phys. Rev. B **87**, 045426 (2013); **88**, 119901(E) (2013).
[55] M. Filipović and W. Belzig, Phys. Rev. B **93**, 075402 (2016).
[56] T. L. Gilbert, Phys. Rev. 100, 1243 (1955); T. Gilbert, IEEE Trans. Magn. **40**, 3443 (2004).
[57] Y. Tserkovnyak, A. Brataas, G. E. W. Bauer, and B. I. Halperin, Rev. Mod. Phys. **77**, 1375 (2005).
[58] D. C. Ralph and M. D. Stiles, J. Magn and Magn. Mater. **320**, 1190 (2008).
[59] C. Kittel, Phys. Rev. **73**, 155 (1948).
[60] A. Fetter and J. D. Walecka, *Quantum Theory of Many-Particle Systems* (Dover Publications, Inc., Mineola, N. Y., 2003).
[61] D. C. Langreth, in *Linear and Nonlinear Electron Transport in Solids*, edited by J. T. Devreese and E. Van Doren (Plenum, New York, 1976).
[62] M. H. Pedersen and M. Büttiker, Phys. Rev. B **58**, 12993 (1998).
[63] Z. Feng, J. Maciejko, J. Wang, and H. Guo, Phys. Rev. B **77**, 075302 (2008).
[64] B. Wang, J. Wang, and H. Guo, Phys. Rev. B **67**, 092408 (2003).
[65] N. Bode, L. Arrachea, G. S. Lozano, T. S. Nunner, and F. von Oppen, Phys. Rev. B **85**, 115440 (2012).
[66] G. Floquet, Ann. Sci. Ecole Normale Supérieure **12**, 47 (1883).
[67] Jon H. Shirley, PhD Thesis, California Institute of Technology, (1963).
[68] M. Grifoni and P. Hänggi, Phys. Rep. **304**, 229 (1998).
[69] S-I. Chu and D. A. Telnov, Phys. Rep. **390**, 1 (2004).
[70] A. Thielmann, M. H. Hettler, J. König, and G. Schön, Phys. Rev. B **68**, 115105 (2003).